Chapter 1

Introduction

The aim of this chapter is to provide a brief background to austempered ductile irons and the chsrscteristics of this material which sre important in understanding the subject.

1.1 Introduction to Austempered ductile irons

Austempered ductile iron (ADI) has a microstructure containing spheroidal graphite embedded in a matrix which is in general a mixture of phases. Of these, bainitic ferrite and austenite are the most desirable phases, but in many cases small amounts of martensite and/or carbides may also be present in the microstructure. The bainitic ferrite is generated during isothermal transformation of austenite at temperatures below the bainite-start (Bs) temperature; this heat treatment is known as "austempering". An optimum combination of high–carbon austenite and bainitic ferrite confers excellent mechanical properties to such cast irons. The proportions of phases change with the chemical composition and heat treatment, making it possible to produce a family of ADIs. This in turn allows a wide range of applications with ADI compiting favourably against steel forgings and aluminium alloys in terms of mechanical properties, manufacturing cost, physical properties, and weight saving [1]. However, much of the development work on ADI has been empirical with the testing of a large number of samples. It is therefore not clear whether the best procedures are currently in place.

The large concentration of silicon typically present in graphitic cast irons has a key

role in the development of the microstructure of austempered irons. The silicon hinders the precipitation of carbides during the bainite transformation [2]. The austempering time must ensure that the formation of bainitic ferrite adequately enriches the residual austenite with carbon, allowing much of it to be retained to room temperature. Unfortunately, prolonged austempering causes the decomposition of the residual austenite into a mixture of carbides and ferrite [3]. This has a detrimental effect on the mechanical properties.

Although ADI was developed during the early 1960's, it could, to some extent still be considered as a new material. This is because despite the huge number of papers and research dedicated to ADI, many of them deal with the routine characterisation of microstructure and mechanical properties with a view to optimising processing. Others consider the role of chemical segregation, and the effect of specific alloying elements. However, a lot less are committed to the application or development of basic theory of phase transformations, for the benefit of ADI. In addition, almost no attention has been dedicated to developing physical or empirical models which allow a quantitative estimation of the microstructure and mechanical properties.

Since ADI is a complex material, it is not easy for the industry to exploit the potential market in different industrial areas, and only specialised parts have been developed using the trial and error method. Models could be of great help since they reduce the exhaustive number of trial and error experiments and can be useful in the design of new products for brand new applications.

The purpose of this research was to develop quantitative models which allow the estimation of the microstructure and mechanical properties of austempered ductile irons as a function of their chemical composition and heat treatment conditions.

1.2 Cast irons

Although the focus of the work in this thesis is about austempered ductile iron, a brief introduction to cast irons is useful since ADI emerged as a new member of the family during the 1960's. The list of cast irons is big and this section describes only the most important ones.

Cast iron is an Fe-C-Si alloy that often contains other alloying elements and is used in the as-cast condition or after heat treatment. Cast irons offer a virtually unique combination of low cost and engineering versatility. The low cost, together with castability, strength, machinability, hardness, wear resistance, corrosion resistance, thermal conductivity, and damping makes them excel even amongst casting alloys [4]. The different types vary from grey iron, which is machinable, to white iron which is not easily machinable. The white irons of suitable composition can be annealed to give malleable cast iron to improve ductility. A simple classification of cast irons is shown in Fig. 1.1. This is based on the form of graphite and the type of matrix structure in which it is embedded [5].

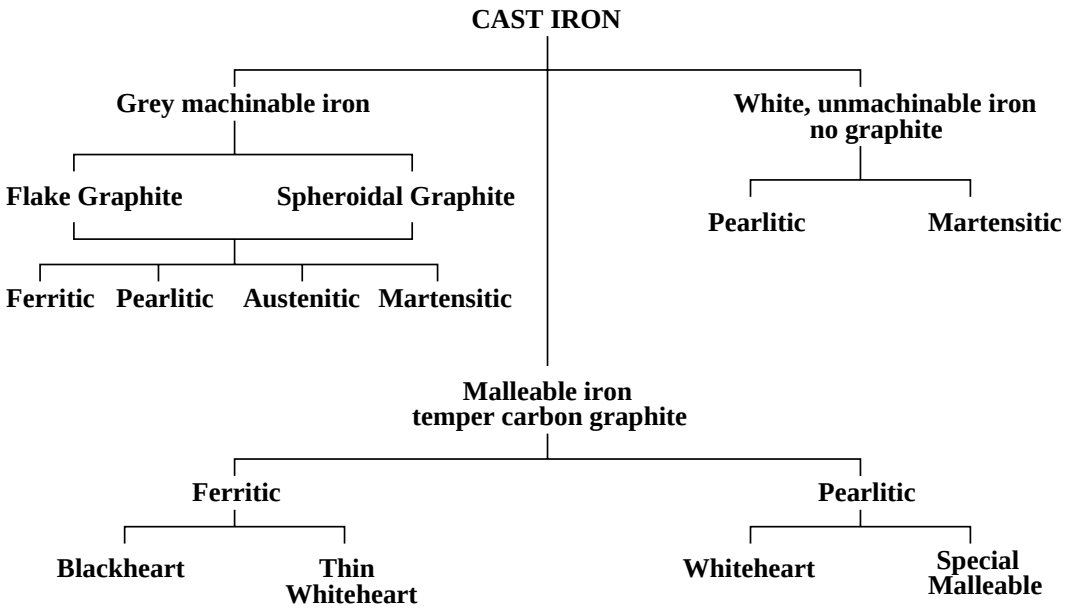

Figure 1.1: Classification of Cast iron [5]

Two factors determine the microstructure (white, ferritic gray, pearlitic gray, etc.) a cast iron will have on solidification. This factors are chemical composition and cooling rate. Fig. 1.2 is a schematic diagram of the effect of carbon and silicon concentrations, and of cooling rate on the microstructure of cast irons [6]. Fig. 1.2 shows that an increase in cooling rate decreases the tendency to form graphite. An increase in the carbon or silicon concentration on the other hand, promotes graphitisation. These obsevations lead to the definition of a carbon–equivalent value (CE) which is an index that indicates the combined effect of elements such as silicon and phosphorus in terms of the influence of carbon. [5] (Fig. 1.3). As the carbon content o CE is reduced below 4.3 wt%, there is a progressive decrease in the amount of graphite, until a mottled or white iron is reached:

$$CE(\text{wt}\%) = C + \frac{(Si + P)}{3} \tag{1.1}$$

For a given cooling rate, the carbon equivalent value (CE) determines how close a given composition of iron is to the eutectic in the Fe-C phase diagram (CE=4.3) and therefore how much free graphite is likely to be present.

Thus, if the cast iron has a CE sufficiently below the eutectic value, possibly because a low silicon content, appreciable quantities of carbide–stabilising elements, or if the cooling rate is sufficiently rapid, graphite is suppressed. The microstructure then consists of primary dendrites of pearlite with interdendritic areas of transformed ledeburite, which is a eutectic mixture of iron carbide and pearlite known as white cast iron [7] Fig. 1.4a. The cementite in white cast irons can be induced to decompose into graphite by prolonged annealing at high temperatures. The final microstructure following heat treatment consists

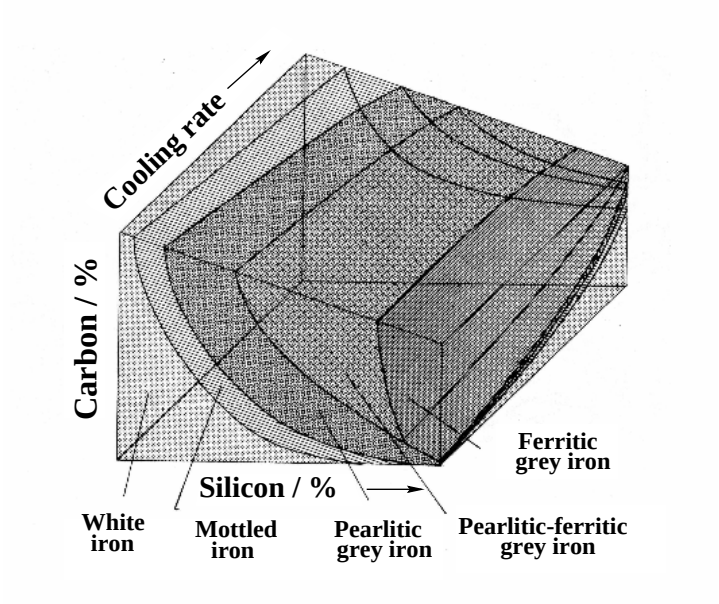

Figure 1.2: The effect of cooling rate and chemical composition on the microstructure of cast iron. Mottled cast irons is a mixture of the white and the gray cast iron microstructures [6]

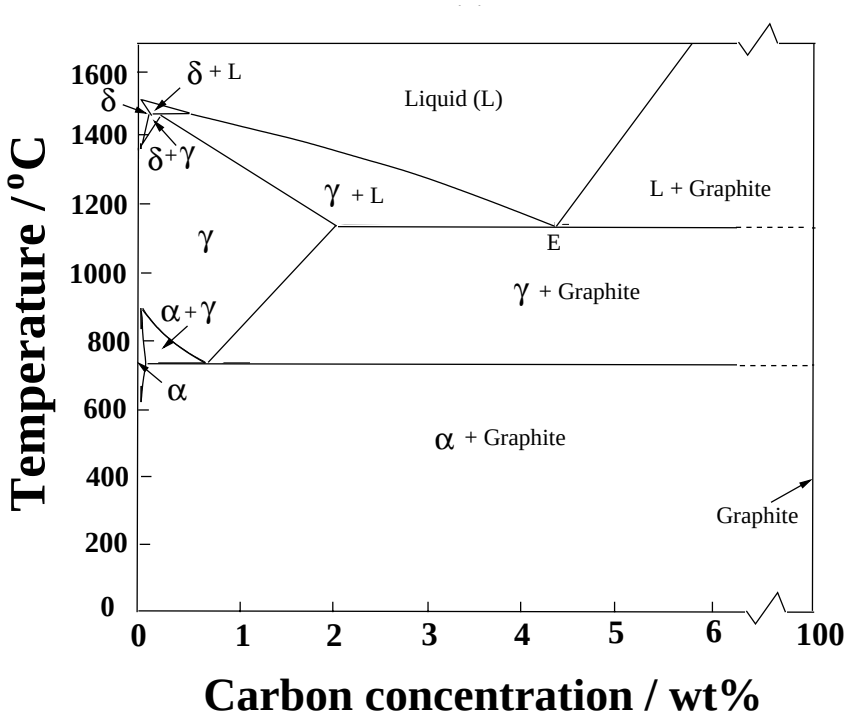

Figure 1.3: The iron-carbon phase diagram. The eutectic point, labelled as "E", corresponds to a carbon content of 4.3 wt%

of graphite distributed in a matrix of ferrite or pearlite. The resulting alloy is called malleable cast iron [6] which for many applications has better mechanical properties than white cast irons which are brittle and hard Fig. 1.4b.

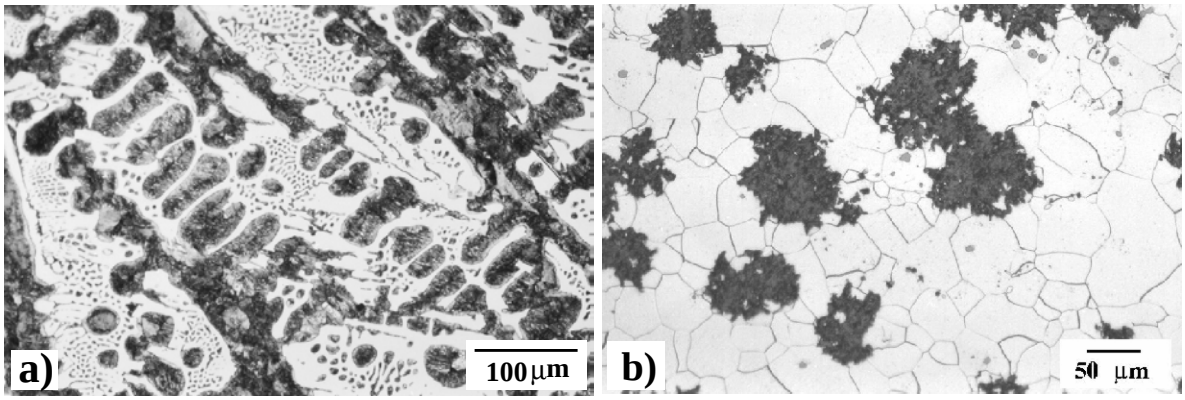

Figure 1.4: Microstructure of a) white cast iron, Fe-3.6C-0.1Si wt%,dendrites of pearlite (from pro-eutectoid austenite) surrounded by areas of pearlite and Fe_3C, b) malleable cast iron produced by heating white cast iron at 900-950°C for many days before cooling slowly. This results in a microstructure containing irregular though equiaxed nodules of graphite in a ferritic matrix. Etchant: 2% nital.

The most common type of cast iron with more than 34 million tons produced in 1999 [8] is grey cast iron. Flakes of graphite form during solidification and the austenite undergoes a eutectoid decomposition into pearlite [6] Fig. 1.5a.

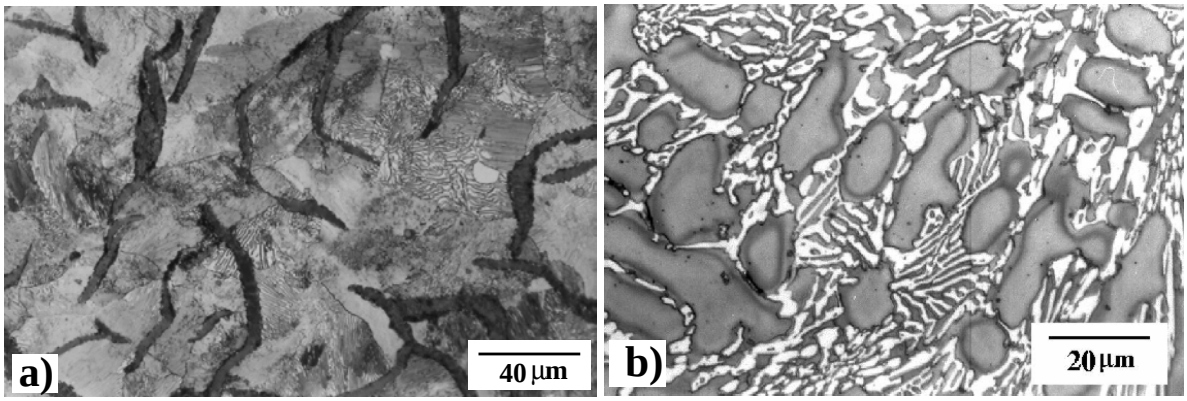

Figure 1.5: Microstructure of grey cast iron, Fe-3.2C-1.1Si wt%, containing graphite flakes in a matrix which is pearlitic. Etchant: Nital 2%, b) wear-resistant high-chromium cas iron, Fe-2.6C-17Cr-2Mo-2Ni wt%. The white phase is a chromium-rich known as M_7C_3. The matrix consists of dendrites of austenite [9]. Etchant: Villela's reagent.

The shape of the graphite precipitated during solidification can be modified markedly. The addition of minute quantities of magnesium or cerium poisons preferred growth directions and leads to isotropic growth resulting in spheroids of graphite. This change in graphite shape gives in an increase in ductility 5 to 20 times greater than grey cast

iron [10]. In addition, as established by Flinn and Kraft [10], the mechanical properties of spheroidal graphite cast irons are determined largely by the matrix, which may be ferritic, pearlitic or a mixture of both as shown in Fig. 1.6a.

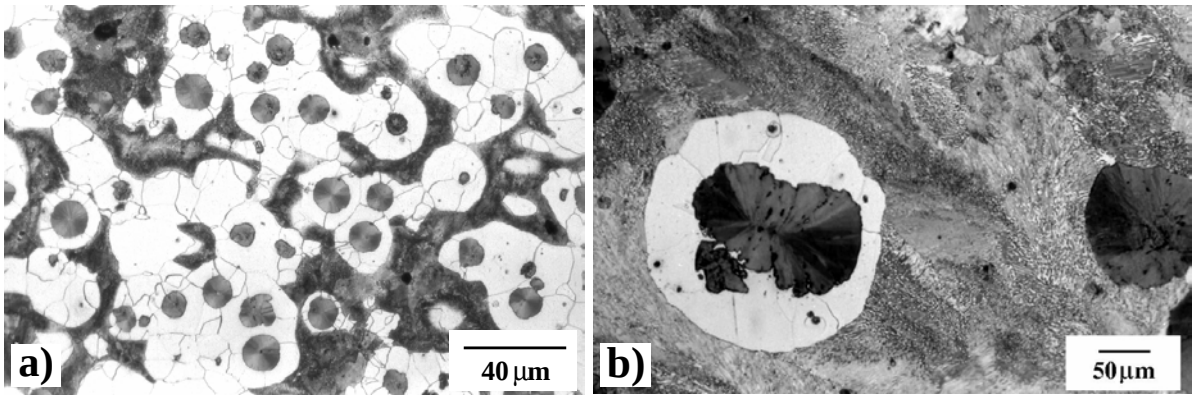

Figure 1.6: Microstructure of a) spheroidal graphite cast iron as-cast, Fe-3.5C-2.5Si-0.5Mn-0.15Mo-0.31Cu-0.042Mg wt%. Nodules of graphite, pearlite (dark islands) and ferrite (light background), b) spheroidal graphite cast iron as-cast, Fe-3.2C-2.5Si-0.05Mg wt% containing graphite nodules in a matrix which is pearlitic. One of the nodules is surrounded by ferrite, simply because the region around the nodule is decarburised as carbon deposits on the graphite. Etchant: Nital 2 wt%.

Speroidal graphite cast irons usually has a pearlitic matrix Fig. 1.6b or a mixture of ferrite and pearlite. however, annealing causes the carbon in the pearlite to precipitate on the existing graphite or to from further small graphite particles, leaving behind a ferritic matrix Fig. 1.7a this gives the iron even greater ductility.

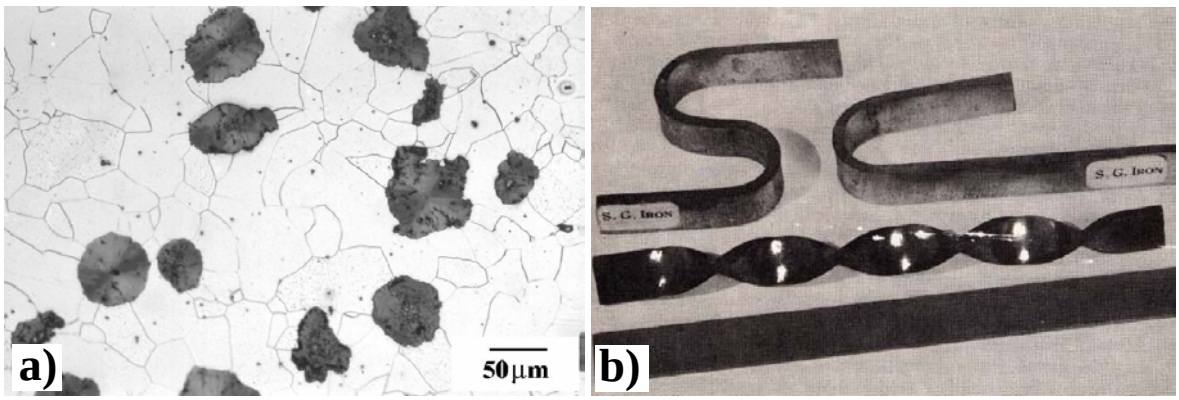

Figure 1.7: Microstructure of a) the same as Fig. 1.6b but annealed. Graphite nodules in a ferritic matrix. Etchant: Nital 2 wt%, b) an illustration of the ductility of spheroidal graphite cast iron [11].

1.3 Austempered Ductile Iron

Since the mechanical properties of spheroidal graphite cast iron essentially depend on the matrix, further enhancements might be achieved by improving the matrix microstructure. The austempering process is an isothermal heat–treatment in the bainitic transformation range, usually 250-450°C. This results in austempered ductile cast iron, with twice the strength of spheroidal graphite cast irons at the same level of toughness and ductility [12]. ADI also has advantages over other materials such as cast or forged steels. This is because ADI has good castability, lower processing cost, higher damping capacity, and a 10% lower density. These characteristics, along with the wide range of mechanical properties that can be achieved via the austempering process, makes ADI competitive for many applications where wrought steels have dominated in the past.

1.3.1 Typical chemical composition

ADI nominally has the chemical composition Fe-3.6C-2.50Si-0.5Mn-0.05Mg wt.%, but a variety of other additions may be made. It is common to see additions of elements such as Mo, Ni and Cu. One reason for alloying is to suppress the pearlite reaction so that the austenite can transform into bainite. Other elements such as chromium and vanadium may be added also to improve hardenability [13], however, this is not common since these are strong carbide-forming elements.

Manganese is a strong promoter of hardenability and its addition is useful to prevent pearlite formation in thick cast–sections. However, since manganese strongly segregates in the intercellular areas between nodules of graphite, causing the precipitation of carbides [14]. It is therefore advisable to keep its average concentration in the range 0.25 to 0.5 wt% [15, 16].

Apart from carbon molybdenum is the most potent hardenability enhancer in ADI (about 1.6 times more than Mn) [3]. However, like manganese, it segregates at cell boundaries during solidification to form carbides [17], so its concentration is usually limited to less than 0.3 wt% [16, 12, 14].

Nickel and copper do not segregate as much as Mn and Mo, and in any case, they partition preferentially into the solid phase [14]. They do not significantly affect the hardenability, but when combined with manganese or molybdenum, there is a useful increase in the maximum section size that can be austempered successfully [3]. Additions of nickel may vary from 0.5 to 3.5 wt%, whereas Cu varies from 0.5 to 1.0 wt%.

There are three important points to consider when selecting the chemical composition of ADI [18];

1. The iron should be sufficiently alloyed to avoid transformation to pearlite, but not over-alloyed to avoid the retardation of the bainite transformation.

2. The microstructure should be free from intercellular carbides and phosphides.

3. The tendency for chemical segregation should be minimised for the sake of uniformity in the cast component.

It has been claimed [3] that small additions of multiple alloying elements is more effective in promoting hardenability than larg amounts of individual alloying elements.

1.3.2 The heat treatment

The austempering process consists of two stages:

1. Austenitisation. The cast component is heated to temperatures between 850 and 950 °C for 15 min to 2 h. In contrast to steels, the austenitising temperature determines the matrix carbon content because the graphite nodules serve as a source or sink for carbon and because the solubility of graphite in austenite increases with temperature.

2. Austempering. After austenitising the cast component is quenched into a salt bath at a temperature in the range 450-250 °C, usually for 0.5 and 3 h, followed by cooling to room temperature.

The temperature of the isothermal transformation is lower than that associated with pearlite but greater than the martensite-start temperature. The heat-treatment produces different types of bainitic microstructures, depending on the temperature and time of treatment. A schematic diagram of the austempering heat treatment cycle is shown in Fig. 1.8

1.3.3 Cooling rate during quenching

The rapid reduction of temperature from the austenitising temperature to the austempering temperature is achieved when the component is placed in the austempering medium. The cooling rate during this stage is of importance since it determines the matrix microstructure of the ductile iron which is to be austempered. A slow quench will tend to produce pearlite; this might occur in large section casting where the central sections experience lower cooling rates compared with the outer regions. Manganese is often added to reduce the rate of pearlite formation during cooling and hence to allow larger castings to be produced. The degree to which bainite can be obtained during the isothermal heat-treatment whilst avoiding pearlite or martensite is known as the 'bainite-hardenability' of an alloy.

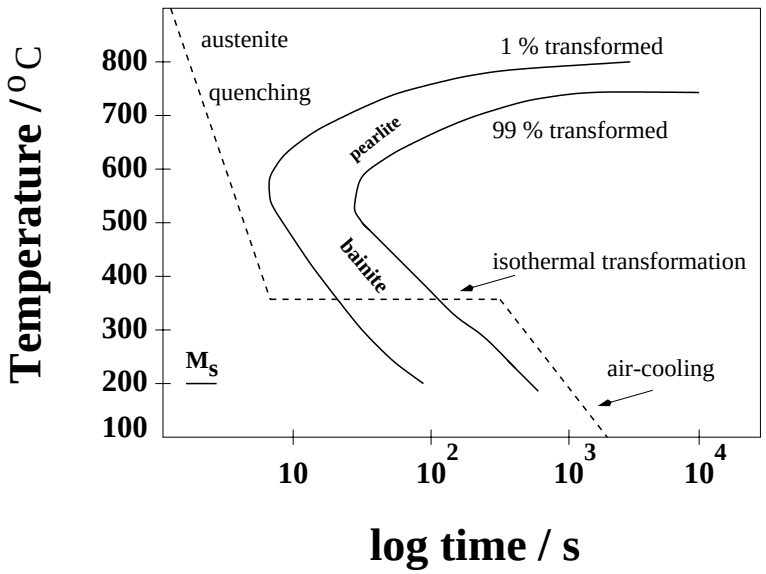

Figure 1.8: Isothermal transformation diagram for an unalloyed spheroidal iron Fe-3.5C-2.5Si-01Mn-0.045Mg with superimposed temperature-time plot typical of an austempering treatment.

1.4 Microstructure of ADI

The austempered microstructure that optimises ductility is a mixture of bainitic ferrite and high-carbon retained-austenite. Other constituents include martensite, carbides and pearlite, all of which tend to reduce ductility. It is difficult during normal processing to avoid these constituents completely, since the composition of the component is rarely uniform.

1.4.1 Upper bainite

The upper bainite consists of fine ferrite plates, each of which is about 0.2 μm thick and about 10 μm long. The plates grow in clusters called sheaves. Within each sheaf the plates are parallel and of identical crystallographic orientation, each with a well-defined crystallographic habit. The individual plates in a sheaf are often called the 'sub-units' of bainite. They are separated by low-misorientation boundaries or cementite particles in the context of conventional steels [19]. Cementite is not found in austempered ductile iron, as well as in high-silicon steels. It is replaced by films of carbon-enriched austenite with or without some metastable carbides such as ϵ or H*ägg* depending on the chemical composition and heat-treatment conditions[19, 20].

1.4.2 Lower bainite

Lower bainite is the predominant morphology in cast irons transformed below 330 °C [21]. It has a microstructure and crystallographic features which are similar to those of upper

bainite. The major distinction is that the transformation is at lower temperature so that carbides can also precipitate inside the plates of ferrite. There are, therefore, two kinds of carbides: those which may grow from the carbon-enriched austenite, and others which precipitate inside the supersaturated bainitic ferrite (Fig. 1.9). In conventional steels these carbides are cementite but in high-silicon steels and in ADI they could be ϵ or other transition carbides. The formation of this microstructure is substantially independent of austempering time and composition.

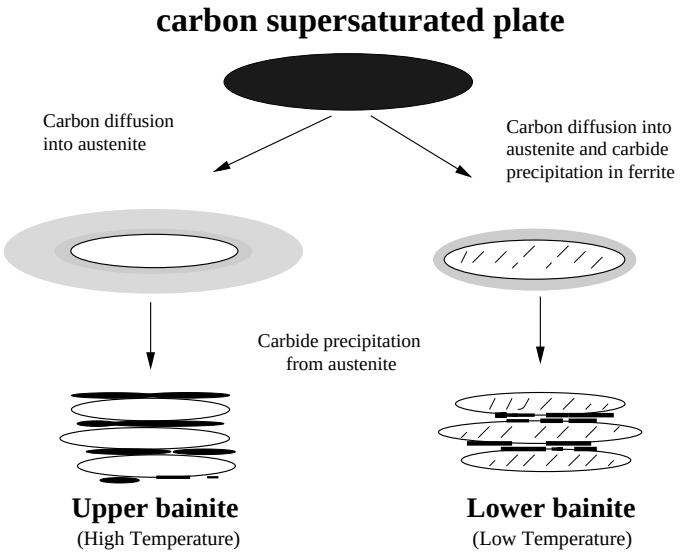

Figure 1.9: Mechanism of formation of lower and upper bainite (Bhadeshia 1992).

1.4.3 Austenite

Austenite is formed during the high temperature step of the heat treatment of ADI. The carbon content of this austenite changes as a function of the austenitising temperature. As a consequence of transformation to bainitic ferrite, the residual austenite becomes enriched with carbon. This reduces the driving force for further transformation [19]. The austenite that is left when the bainite transformation ceases is stabilised by the carbon enrichment and hence can be retained at room temperature. The volume fraction of retained austenite can be as high as 0.6 [22].

When discussing the microstructure, it is necessary to distinguish between *residual austenite*, which exists at the isothermal transformation temperature, and *retained austenite* which remains untransformed at ambient temperature.

1.4.4 Martensite

Some of the carbon-enriched residual austenite may transform into martensite on cooling to room temperature Fig. 1.10.

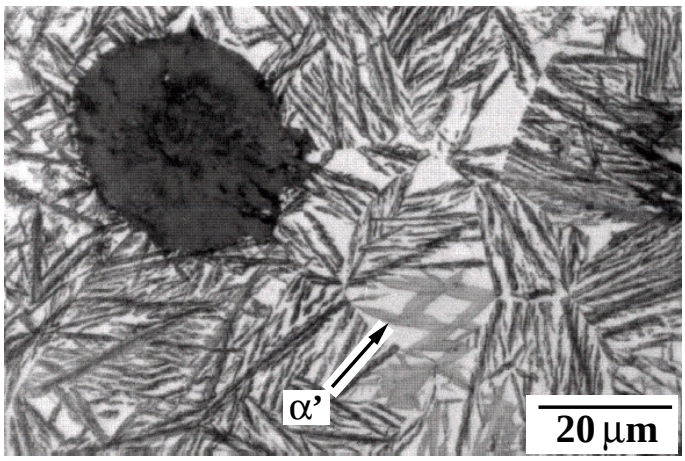

Figure 1.10: Microstructure of ADI showing graphite, and a mixture of upper bainitic ferrite (dark sheaves), retained austenite (light phase), and some martensite (α ') inside retained austenite area.

1.4.5 Carbides

It is silicon which hinders the precipitation of cementite in which it has a very low solubility [2]. Thus, transition carbides precipitate either in austenite or in bainitic ferrite depending on the chemical composition and heat treatment [23]. Prolonged austempering can cause the decomposition of the residual austenite into a mixture of carbides and ferrite [3]. This is detrimental to mechanical properties.

1.5 The processing window

The austempering process is conventionally defined in two stages [24]. The end of the first stage corresponds to the maximisation of the fraction of bainitic ferrite and the enrichment of the austenite, the second with the onset of carbide precipitation. The time interval between these two stages is the heat treatment window (Fig. 1.11). During this interval, only minor changes in the morphology and composition of the ferrite and stabilised-austenite microstructure take place [3]. The extent of this heat-treatment window depends on many factors, including the chemical composition, segregation patterns, and the austempering and austenitising temperature [12]. Manganese has a strong effect and high contents of this element can effectively shrink or even eliminate the heat-treatment window due to overlap of stage I and II [25]. A closed processing window (Fig. 1.11) means that the optimum mechanical properties cannot be achieved due to the severity of the overlap. Martensite occurs in regions with less carbon-enrichment of austenite, and carbides in those regions where stage II has started prematurely because of chemical segregation.

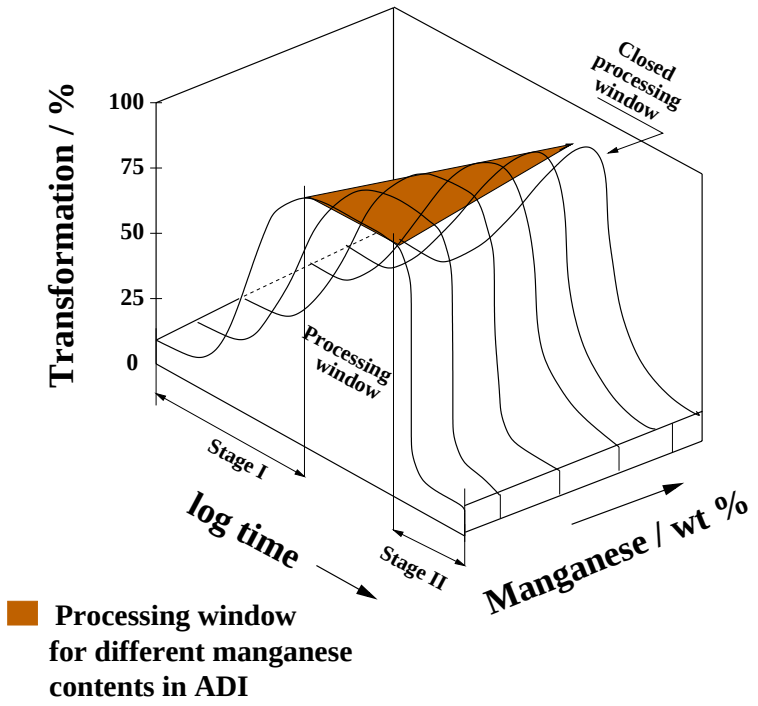

Figure 1.11: Schematic representation of the heat-treatment processing window and the influence of manganese.

1.5.1 Segregation

All the alloying elements segregate between the liquid and solid phases during solidification. This can strongly influence the processing window and, therefore, the mechanical properties. The distribution of alloying elements is related to the eutectic cell that forms around the nodules of graphite during solidification, and leads to a different response in transformation kinetics as a function of position. Three zones along the eutectic cell have been designated to illustrate the distribution of elements in ductile irons [26, 27] Fig. 1.12.

1. Zone I is located along the graphite. In this zone the silicon, nickel and copper levels are high but the manganese is depleted.

2. Zone II represents the greater part of the matrix where the change in solute concentration is more gradual.

3. Zone III is located at the solidification cell boundary. The silicon and copper levels are low but manganese, molybdenum, chromium and phosphorus are enriched.

1.6 Mechanical properties

Austempered ductile irons can have tensile strengths of up to 1700 MPa with about 1.7% elongation (Table 1.1) and high hardness, for applications in which wear resistance is of

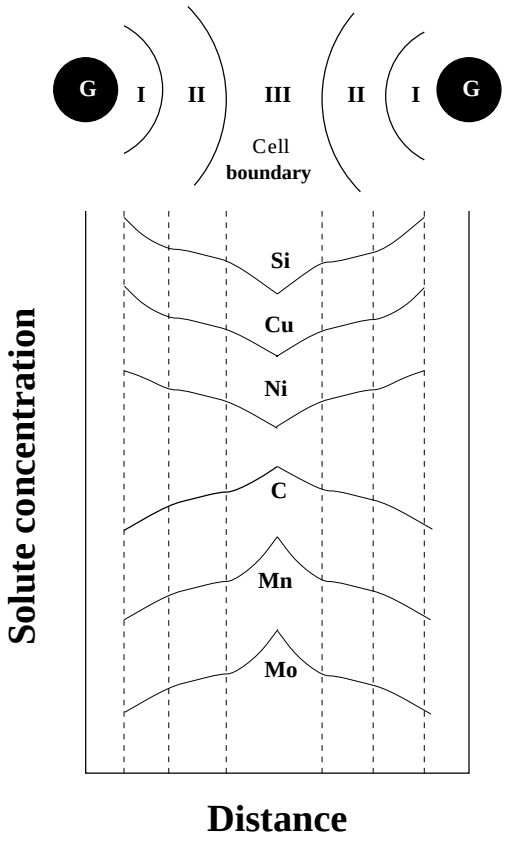

Figure 1.12: Solute segregation zones between adjacent graphite nodules.

primary importance. Materials of lower hardness having tensile strengths between 900 to 1200 MPa and elongation of up to 16% can also be produced, for engineering applications where ductility is vital [15, 28]. For practical purposes, there are two types of ADI:

1. Class I: ductile irons transformed at low austempering temperatures exhibiting a lower bainite matrix. These irons have high hardness ($\geq$ 400 HB) and strength, and are particularly desirable for gears and other applications requiring resistance to high contact stress.

2. Class II: ductile irons transformed at high austempering temperatures exhibiting upper bainite. These irons have hardnesses ranging from 260 to 350 HB. They combine high ductility and toughness with high fatigue strength and wear resistance. They are reasonably machinable and are commonly used in structural applications [29].

It has been suggested that development of the unique combination of strength and ductility in ADI is a result of the presence of the relatively continuous high carbon austenite matrix [30].

The British standards specification (BS-EN-1564) for ADI is shown in Table 1.2 with minimum acceptable values. These values can be compared with data shown in Table 1.1.

Main elements wt.%	T_γ °C	t_γ min	T_a °C	t_a min	UTS MPa	Elongation %	Reference
3.6C-2.5Si-0.45Mn-0.75Ni-0.5Cu	871	90	260	90	1707	1.7	Kovacs, 1988
3.56C-2.63Si-0.15Mn-0.45Ni-0.44Cu	900	90	300	180	1602	1.7	Lin, 1996
3.44C-2.41Si-0.15Mn	898	120	302	120	1510	2.8	Putatunda, 1999
3.8C-2.6Si-0.25Mn-0.1Mo	897	60	297	60	1500	4	Takahashi, 1996
3.6C-2.7Si-0.2Mn-0.28Mo-0.6Ni-0.6Cu	970	60	343	60	1250	9	Stenfors, 1986
3.4C-2.95Si-4.83Ni	900	20	300	120	1352	10	Aoyama, 1996
3.56C-2.8Si-0.96Ni	900	30	375	30	1169	16.6	Varahraam, 1990

Table 1.1: Some examples of mechanical properties, UTS and elongation as a function of chemical composition and heat treatment conditions in ADI. T_γ= *Austenitising temperature,* t_γ= *Austenitising time,* T_a= *Austempering temperature,* t_a= *Austempering time.*

Material identification	Number	Tensile strength MPa (min)	0.2% Proof stress MPa (min)	Elongation % (min)
EN-GJS-800-8	EN-JS1000	800	500	8
EN-GJS-1000-5	EN-JS11100	1000	700	5
EN-GJS-1200-1	EN-JS1120	1200	850	2
EN-GJS-1400-1	EN-JS1130	1400	1100	1

Table 1.2: British Standards specification for ADI EN-1564:1997

1.7 Applications of ADI

Before indicating some applications of ADI it is important to remember some physical characteristics, which combined with the mechanical properties of ADI, open the market for this material in many different industries, but particularly for automotive components.

1. Good castability and near net shape casting production of parts.
2. 10% lower density than steel.
3. Higher damping capacity than steel which makes the parts to absorb energy 2-5 times more than steels, thereby reducing the level of noise to about 8-10 decibels in gear boxes [31, 32].

The combination of these characteristics with the austempering process creates a big family of ADIs which can compete with forging steels and even with aluminium parts [1], not only in the mechanical performance but also in the cost of production. Examples of applications are:

1. Automotive: crankshafts, camshafts, hypod pinion and ring gear pairs, and timing gears for diesel engines Fig. 1.13.

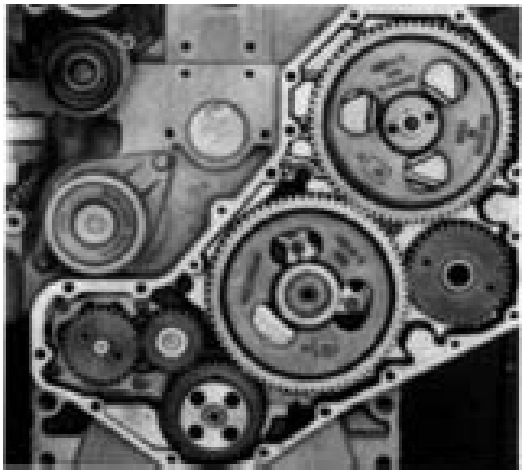

Figure 1.13: Timing gears for diesel engines. ADI has been chosen in preference to induction hardened AISI 4140 steel. These ADI gears were austempered at 238°C to give a high hardness [33].

2. Heavy trucks: spring hangar brackets, "U"-bolt plates, pivot pins, clip plates, connecting-rods, engine mounts and gears.

3. Railroads: side bearing top caps, track plates, motor nose supports, pick-up arms, rail braces and suspension components.

4. Mining: sprockets, chains, chain guides, track trends, wear plates,

5. Pumps and compressors: impellers, valve bodies, compressor housings, gears and drilling heads.

6. Construction equipment: track guides, hydraulic cylinders, track shoes, adjustment cams, rock guards, pin covers, backhoe digger teeth, circle drive gears, bearing caps, and support arms

Since the potential of ADI is enormous, it is important to know all the mechanisms involved in the production of optimum ADI parts. This may give industry better tools to exploit the market which has for some time been reluctant to use ADI, partly due to the difficulties in controlling all the variables. The creation of physical and empirical models can contribute enormously in the improvement and design of new components.

References

[1] Rimmer A. A.d.i. is growing. *Materials World*, pages 252–255, 1997.

[2] Owen W. S. The effect of silicon on the kinetics of tempering. *Transactions of the ASM*, 46:812–829, 1954.

[3] Voigt R. C. Austempered ductile iron-processing and properties. *Cast Metals*, 2:72–93, 1989.

[4] Elliott R. *Cast Iron Technology*. Butterworths & Co.(publishers) Ltd, 1988.

[5] Rollason E. C. *Metallurgy for Engineers*. Edward Arnold Ltd, 4th edition edition, 1973.

[6] Guy A. G. *Elements of Physical Metallurgy*. Addison-Wesley Publishing Company, Inc., 2nd edition edition, 1960.

[7] Angus H. T. *Cast iron: Physical and engineering properties*. Butterworths & Co. (publishers) Ltd, 2nd edition edition, 1976.

[8] A Modern casting Staff Report. 34th annual census of world casting production-1999. *Modern casting*, 2000.

[9] Bedolla-Jacuinde A. Microstructure of vanadium-niobium and titanium-alloyed high-crhomium white cast irons. *International Journal of Cast Metals Reseach*, 13:343–361, 2001.

[10] Flinn R. A. and Kraft R.W. The interrelation of mechanical properties, section siza and microstructure of ductile cast iron. *Transactions ASM*, 44:282–306, 1952.

[11] Petty E. R. *Physical Metallurgy of Engineering Materials*. George Allen and Unwin Ltd, 1970.

[12] Rundman K. B. Moore D. J. Hayrynen K. L. Dubensky W. J. and Rouns T. N. The microstructure and mechanical properties of austempered ductile iron. *Journal of Heat Treating*, 5:79–95, 1988.

[13] Singh I. and Putatunda S. K. Fatigue crack growth behaviour of austempered ductile cast iron (adi) alloyed with chromium. *Transactions of the Indian Institute of Metals*, 47:317–325, 1994.

[14] Dorazil E. *High Strength Austempered Ductile Cast Iron*. Series Editor: E.G. West, Obe. Horwood Series in Metals and Associated Materials, 1991.

[15] Harding R. A. Prospects for the exploitation of austempered ductile irons. In *Proceedings, 2nd International Conference on Austempered Ductile Iorn*, pages 39–54, Ann Arbor, MI, USA, March 17-19 1986.

[16] Rouns T. N. and Rundman K. B. The constitution of austempered ductile iron and the kinetics of austempering. *AFS Transactions*, 95:851–874, 1987.

[17] Trudel A. and Gagne M. Effect of composition and heat treatment parameters on the characteristics of austempered ductile irons. *Canadian, Metallurgical, Quarterly*, 36:289–298, 1998.

[18] Morgan H. L. Introduction to foundry production and control of austempered ductile irons. *The British Foundryman*, pages 98–108, 1987.

[19] Bhadeshia H. K. D. H. *Bainite in Steels*. The Institute of Materials, 1992.

[20] Rundman K. B. Dubensky W. J. An electron microscope study the carbide formation in austempered ductile iron. *AFS Transactions*, 93:389–394, 1985.

[21] Harris D. A. Tech B. and R.J. Maitland. The products of the isothermal decomposition of austenite id a spheroidal graphite cast iron. *Iron and Steel*, pages 53–60, 1970.

[22] Klug R. C. Rundman K. B. An x-ray and metallographic study of an austempered ductile cast iron. *AFS Transactions*, 90:499–508, 1982.

[23] Arnould J. Schissler J. M. and Metauer G. Etude de la dcomposition de l'austnite post-bainitique d'alliages fer-carbone-silicium a 1% de manganse. *Mmoires Scientifiques Revue Mtallurgie*, pages 779–793, 1975.

[24] Rouns T. N. Moore D. J. and Rundman K. B. Effect of manganese on structure and properties of austempered ductile iron: A processing window concept. *AFS Transactions*, 94:255–264, 1986.

[25] Darawish N. and Elliott R. Austempering of low manganese ductile irons part 1-processing window. *Materials Science and Technology*, 9:572–585, 1993.

[26] Bak C. Schissler J. S., Chabaut J. and Gouvenel D. Stability of adi structures at room temperatures. In *2nd International Conference on Austempered Ductile Iro*, pages 149–155, Ann Arbor, MI, USA, March 17-19 1986.

[27] Bayati H. and Elliott R. Austempering process in high manganese alloyed ductile cast iron. *Materials Science and Technology*, 11:118–129, 1995.

[28] Yanagisawa O. Varahraam N. Properties of austempered ductile iron in equipment designed for consecutive in-stream treatment gravity-diecasting, and direct austempering. *Cast Metals*, 3:129–139, 1990.

[29] Gundlach R. B. and Janowak J. Austempered ductile iron combines strength with toughness and ductility. *Metal Progress*, pages 19–26, 1985.

[30] Lin. C. K. and Hung T.P. Influence of microstructure on the fatigue properties of austempered ductile irons–ii low-cycle fatigue. *International Journal of Fatigue*, 18:309–320, 1995.

[31] Rossi F. S. and Gupta B. K. Austempering of nodular cast iron automobile components. *Metal Progress*, pages 25–31, 1981.

[32] Salonen P. The environmentally improved design of truck axle hub with austempered ductile iron kymenite-adi. In *International Conference on Engineering Design ICED 97*, pages 637–640, Tampere, August 1997.

[33] Internal Report. Selected case studies of austempered ductile iron components. Technical report, British Cast Iron Reseach Asociation (BCIRA).